

INTERACTING DAMAGE MODES IN TITANIUM-GRAPHITE HYBRID LAMINATES

Dennis A Burianek, and S. Mark Spearing

*Technology Laboratory for Advanced Composites, Massachusetts Institute of Technology,
Cambridge, MA 02139, USA*

SUMMARY: An experimental and analytical investigation was conducted of the growth under cyclic loading of face-sheet cracks coupled with delaminations in titanium-graphite hybrid laminates. A 3-D finite element model was developed to obtain the stress-intensity factor for the titanium face-sheet crack as a function of the material properties, ply thicknesses, specimen geometry and delamination shape. The results for the stress-intensity factor were compared to a 2-D finite element model and a cohesive zone/bridged crack model. Significant differences were identified indicating that for this problem it is essential to use a full 3-D analysis. The model was applied to experimental data for three laminates (Ti/0/90/0₂)_s, (Ti/90/0/90₂)₂ and (Ti/0/90/±30)_s. An independently-calibrated Paris Law was used to describe the fatigue crack growth behavior of the face-sheets. A good description of the experimental data was obtained for the first two laminates, with a slightly less-good description for the third. This poorer fit was attributed to the presence of additional damage modes in the laminate containing ±30° plies. In all cases the face-sheet cracks were found to asymptote to a steady state (crack length-independent) growth regime, which was predicted by the 3-D finite element model. Crack opening displacement profiles measured experimentally were compared with those predicted by the finite element model. Good agreement was demonstrated, indicating that the FE model correctly modeled the load transfer mechanisms around the crack.

KEYWORDS : Fatigue crack growth, Delamination, Modeling, Hybrid Laminates

INTRODUCTION

Titanium-graphite hybrid laminates are being developed for high-temperature aerospace applications [1]. Hybrid laminates such as TiGr, sometimes called fiber metal laminates (FML), are made of polymer matrix composite (PMC) plies interspersed with metal foil. The two materials are assembled by bonding the PMC plies and metal foils to form a composite laminate. Previous work using TiGr [2] investigated the elevated temperature (177° C) fatigue damage modes in TiGr laminates with open holes and identified the growth of cracks in the facesheets coupled with delamination as the key damage modes contributing to stiffness reduction. In addition, it was shown that the stiffness decreases more rapidly at elevated temperatures than at room temperature. Marrissen [3] and Lin et. al. [4] investigated the crack growth behavior of the metal plies in an ARALL laminate for center cracked tension panels and single edge notch tension panels, respectively. Guo and Wu [5] also conducted studies on the crack growth behavior in GLARE laminates. The work described in this paper will build upon the previous work to develop a model for facesheet crack growth and compare the predictions to experimental data. A fuller description of the work described in this paper can be obtained from references [6-9]

MODELING

A schematic diagram of the problem under consideration is shown in figure 1. The facesheet crack is accompanied by a delamination.. A hierarchical (global-local) finite element model

for this geometry was constructed in ABAQUSTM. 8 node brick elements were used throughout. Appropriate material properties were assumed for the titanium and the composite core (see table 1, in the experimental section). A relatively coarse model was constructed of the full width of the specimen and half the thickness (exploiting symmetry). The loads and displacements around the crack tip region were exported to a more refined local model of the crack tip region. The virtual crack-closure technique (VCCT) was then applied to obtain the stress intensity factor at the crack tip.

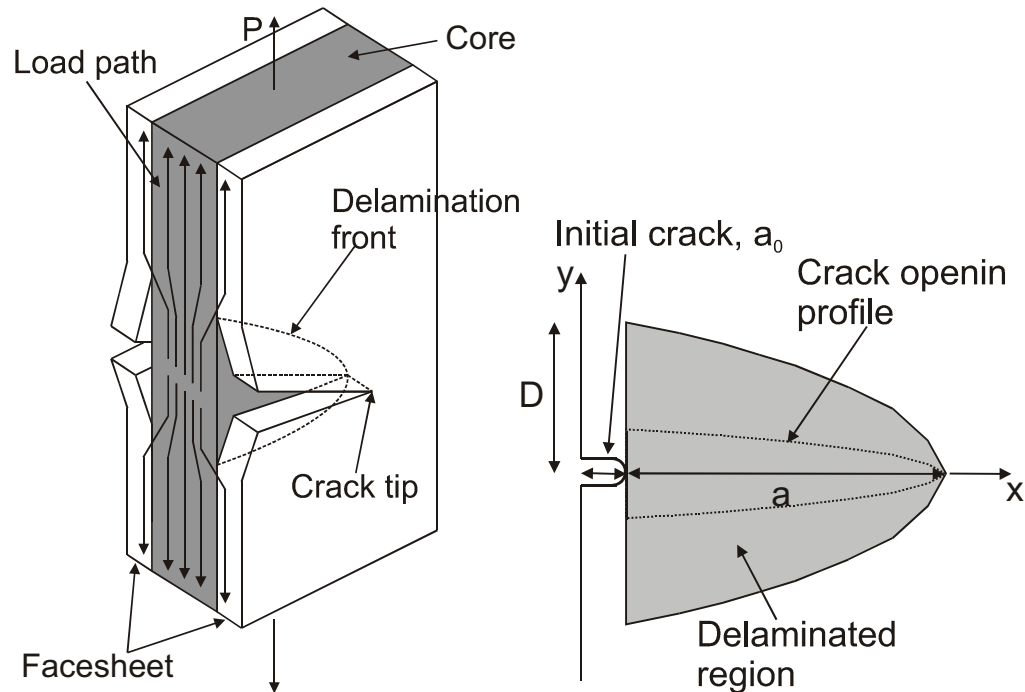


Fig. 1 Schematic diagram of facesheet crack accompanied by delamination

Results for the stress intensity factor (normalized by the ply thickness and applied stress) for four delamination aspect ratios and shapes are shown in figure 2. It is apparent that the delamination shape has a strong influence on the crack tip stress intensity factor. It is also interesting to note that for cracks more than about 10 mm long the stress intensity factor becomes independent of the crack length, indicating that the controlling dimension is the facesheet thickness modified by the elastic properties and dimensions of the core. This is characteristic of steady state, tunneling, crack behavior.

Previous efforts to model this class of problem have employed cohesive zone, or bridge crack models [3-5], in which the effect of the intact composite plies is represented by a distribution of bridging tractions acting on the crack surface. A model, closely based on that of Marissen [4] was implemented, in which an elliptical delamination was assumed. In addition a 2-D finite element was constructed in which no out of plane effects were included. Figure 3 compares the results of the three modeling strategies. It is clear that the bridged crack (BC) model does not correlate with the 3-D FE VCCT model. Furthermore, the 2-D FE VCCT model, agrees with the 3-D model regarding the trend in stress intensity factor with crack length, but tends to underpredict the stress intensity factor (although it is significantly closer to the 3-D results than the bridged crack model). The two key reasons for these discrepancies are that the out of plane stresses and strains and their through-thickness variations are important contributions to determining the stress intensity factor and these are not modeled in either the bridged crack model or the 2-D FE VCCT model. In addition the calculated stress intensity factor is very sensitive to the details of the delamination shape near the crack tip.

These details are not well captured by the bridged crack model. These discrepancies may have important ramifications for the modeling of other damage problems in composite laminates.

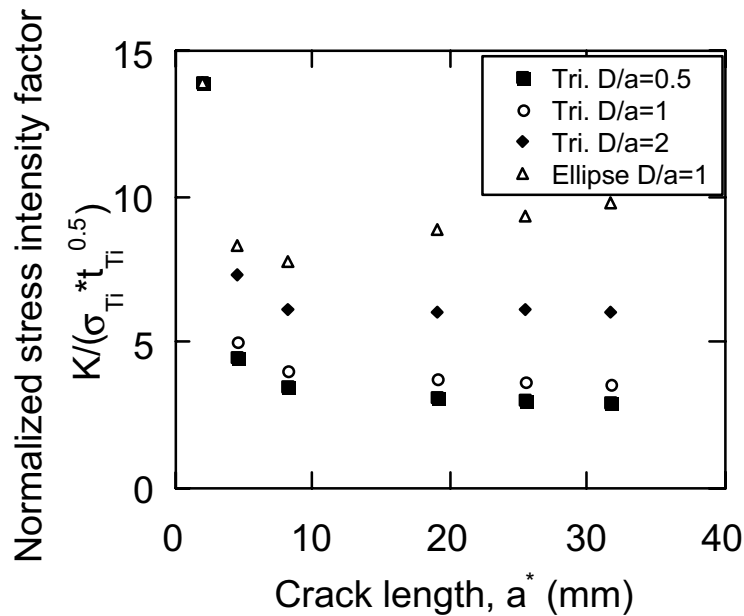


Fig. 2 Effect of delamination shape on crack tip stress intensity factor.

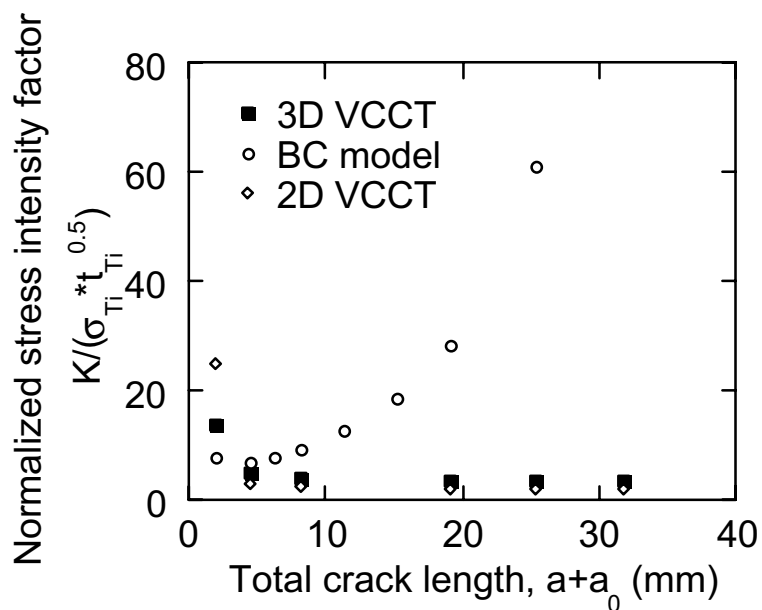


Fig. 3 Effect of delamination shape on crack tip stress intensity factor.

In order to compare the models with experimental data a fatigue crack growth law for the titanium facesheets was assumed, based on data obtained for monolithic Ti15-3-3-3. This was fitted by a simple power law (Paris Law) relationship. In combination with the stress intensity factors calculated from the 3-D FE VCCT model, this allowed predictions of the crack growth rate to be made.

EXPERIMENTAL METHOD

The test specimens were 152 mm x 38 mm rectangular coupons. The specimen lay-up for the base laminate was $[\text{Ti}/0/90/0_2]_s$. The titanium layers were made from the meta-stable beta titanium alloy, 15V-3Cr-3Al-3Sn (Ti 15-3), 0.127 mm in thickness. The polymer matrix composite plies were 0.142 mm in thickness and contained IM7TM graphite fibers and the thermoplastic matrix, PIXA-M. Two alternate lay-ups were also tested: $[\text{Ti}/90/0/90_2]_s$ and $[\text{Ti}/0/90/\pm 30]_s$. Material properties for the constituent materials and for the laminates are given in Table I. The coefficient of thermal expansion for the titanium alloy is $8.64 \cdot 10^{-6}/^\circ\text{C}$. The coefficient of thermal expansion for the composite lamina is $0.9 \cdot 10^{-6}/^\circ\text{C}$ in the longitudinal (fiber) direction and $4.5 \cdot 10^{-6}/^\circ\text{C}$ in the transverse direction. All the specimens had a 2 mm long notch in the edge of the specimen located along the centerline of the specimen. The notch was cut using a 0.64 mm diameter diamond grit end mill.

Table 1. Material Properties

Material Property	Ti 15-3	IM-7/ PIXA-M	TiGr $[\text{Ti}/0/90/0_2]_s$	TiGr $[\text{Ti}/90/0/90_2]_s$	TiGr $[\text{Ti}/0/90/\pm 30]_s$
E_1 (GPa)	107	155	118	58.5	86.9
E_2 (GPa)	112	6.9	58.5	118	59.6
G_{12} (GPa)	41.4	5.1	11.7	11.7	22.3
ν_{12}	0.33	0.35	0.16	0.08	0.32

Fatigue tests were carried out using a servo-hydraulic load frame with a sinusoidal waveform under load control. Damage observation was performed using a long distance microscope system. The stage for the microscope was equipped with digital position encoders along all space dimensions, which allowed for measurement of the crack length without removing the specimen from the load frame. The fatigue cycling was interrupted and the load was held at the mid-point of the fatigue cycle in order to measure the crack length. Although the cracks did not propagate along a perfect horizontal line, only the lateral distance was recorded and the small vertical component was ignored.

The delamination profile was tracked using x-radiography. The specimen was held at a constant load and injected with a di-iodobutane solution and removed from the load frame to be x-rayed in an x-ray cabinet. In addition, post-mortem analysis of the delamination profile was conducted by spraying the laminate with die penetrant and allowing it to flow into the damaged regions. A developing fluid was then applied to the specimen to remove any excess die penetrant. The facesheet was carefully removed to reveal the extent of the delamination. Additional details of the experimental procedures are included in references [7] and [8].

RESULTS

The fatigue crack growth rate as a function of the applied stress intensity factor in the facesheet for the base laminate, $[\text{Ti}/0/90/0_2]_s$, is shown in Figure 4 for three applied stress levels, $\sigma_{\text{max}}=314$ MPa, $\sigma_{\text{max}}=419$ MPa, and $\sigma_{\text{max}}=524$ MPa. The results show that as the crack extends, i.e. for increasing values of the applied stress intensity factor (calculated on the basis of the applied load and measure crack length), the crack growth rate approaches a constant

value. This is consistent with the 3D FE VCCT modeling results. The crack growth rate corresponding to the results of the 3D FE model for a delamination to crack ratio, D/a , of 1 is also shown in Figure 4. The predictions from the 3D VCCT model have very good correlation with the experimental results. Beyond the assumption of $D/a=1$ the results of the 3D VCCT model have no additional tuning or adjustment. For comparison, the crack growth rate profile from the Paris' law relationship for monolithic titanium 15-3-3-3 is also shown in Figure 4. For the monolithic material, the crack growth rate increases as the crack extends, as opposed to the initially decreasing and then steady-state behavior predicted and observed for TiGr laminates. The crack growth rate for the TiGr laminate is several orders of magnitude lower than that for monolithic titanium, illustrating the potential of TiGr laminates for applications in which fatigue damage resistance is a key consideration.

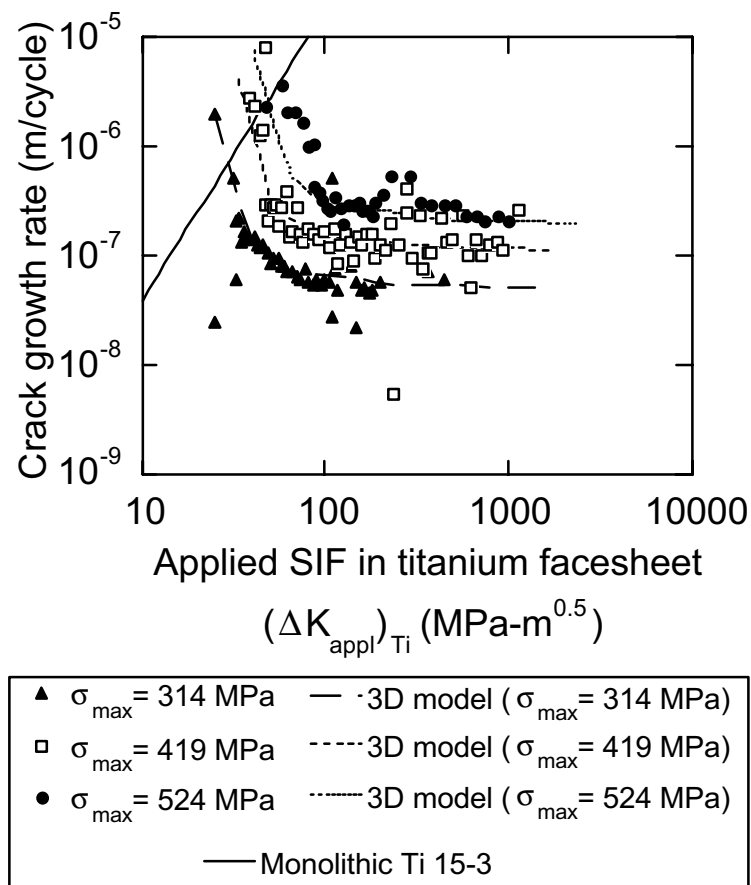


Figure 4. Comparison of model predictions and experimental data for $(\text{Ti}/0/90/0_2)_s$ loaded at three stress levels, $R=0.1$.

One of the assumptions of the model was that the delamination growth was self-similar and had an aspect ratio (D/a) of approximately 1. In order to investigate the validity of this assumption, destructive evaluation was conducted on the specimens after the completion of the fatigue cycling. Die penetrant was sprayed onto the specimen and allowed to wick into the delaminated areas. Once dried, the facesheet was removed from the core and the furthest extent of the delamination was assessed based on observations of the residue left by the die penetrant. Figure 5 illustrates the delamination profiles from three specimens with different final crack lengths. The delamination profiles were approximately triangular for a majority of the specimens and the angle with respect to the facesheet crack ranged from 30° to 45° (45° corresponds to $D/a=1$ in the 3D model). There is a trend indicating that the delamination angle remains closer to 45° for shorter cracks and decreases as the crack length extends,

possibly reflecting a decreased influence of the free edge for longer cracks. It is important to note that the delamination aspect ratio used in the modeling was chosen based on experimental observations. Work is underway to develop the means to predict independently the delamination shape.

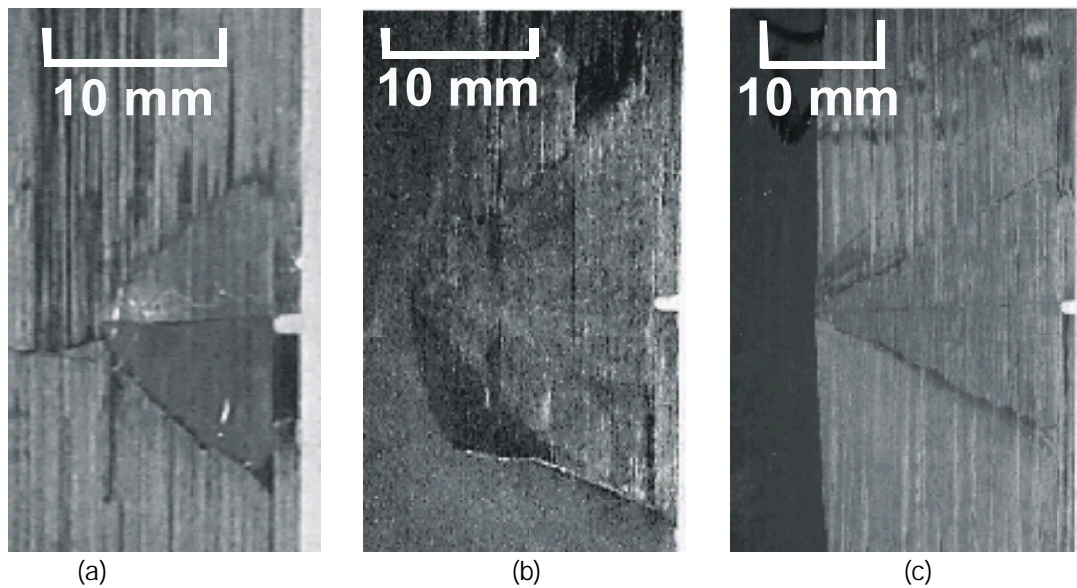


Figure 5. Delamination geometry revealed by use of a penetrant at (a) $a=8.7$ mm, (b) $a=19$ mm and (c) $a=23$ mm.

To verify that the finite element model was accurately capturing the load transfer mechanism between the intact composite core and the cracked and delaminated titanium facesheet, a comparison was conducted between the predicted crack opening displacement from the 3D finite element model and the experimental results. To obtain the experimental crack opening profile, an acetate replication procedure was used. At a total crack length, a^* , of 16 mm, the cycling was interrupted and a replicate was taken of the crack opening with the specimen held at a constant stress level. To obtain the replicate, a strip of 25 mm wide acetate film was cut to the appropriate length and held against the surface of the specimen. A small amount of acetone was applied to the side of the acetate tape facing the specimen and the tape was carefully pressed against the specimen over the cracked region, including the initial notch. After the acetone had dried, the tape was slowly removed and placed between microscope slides for observation. The replicate was initially inspected for smudges or contamination and if either had occurred, the procedure was repeated until a good quality replicate was obtained.

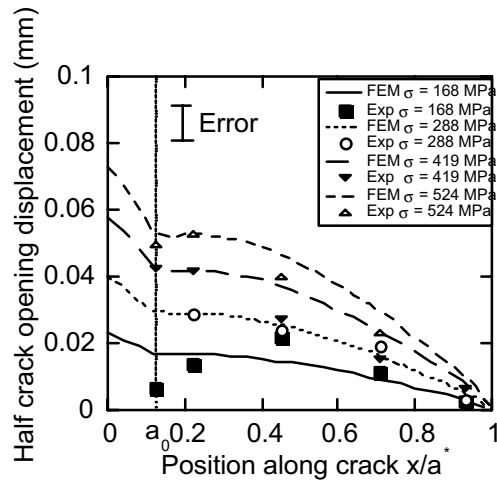


Figure 6. Comparison of experimentally measured crack opening displacement and that predicted by the 3D FE model.

Replicates were taken at each of 5 different laminate stresses, 0 MPa, 168 MPa, 288 MPa, 419 MPa, and 524 MPa. Each of the replicates was studied under an optical microscope at approximately 200x magnification. The crack opening displacements were recorded along the crack length for each applied stress level. The measurements were performed using the ZeissTM KS-300 software package. The residual crack opening displacement at 0 MPa was subtracted from the results at the higher stress levels to determine the net crack opening displacement profile as a function of the applied stress. The results are compared to the finite element results in Figure 6. There is good agreement between the 3D finite element results and the experimental results, indicating that the finite element model is capturing the load transfer mechanism across the facesheet crack. Such independent observations of local deformations are an important part of the validation of a physically-based model, such as the one presented here.

Fatigue experiments were also conducted on TiGr laminates with lay-ups of $[Ti/90/0/90_2]_s$ and $[Ti/0/90/\pm 30]_s$. The experiments were conducted so that the far-field stress level in the facesheet ply matched that of the experiments on the base laminate. The fatigue crack growth behavior as a function of the applied facesheet stress intensity factor for three different applied stress levels is shown in Figure 6 for the $[Ti/90/0/90_2]_s$ laminate. The experimental results for the $[Ti/90/0/90_2]_s$ laminate indicate a slightly higher steady-state growth rate as compared to the base $[Ti/0/90/0_2]_s$ laminate. Again the 3D VCCT model provides a reasonable estimate for the crack growth behavior.

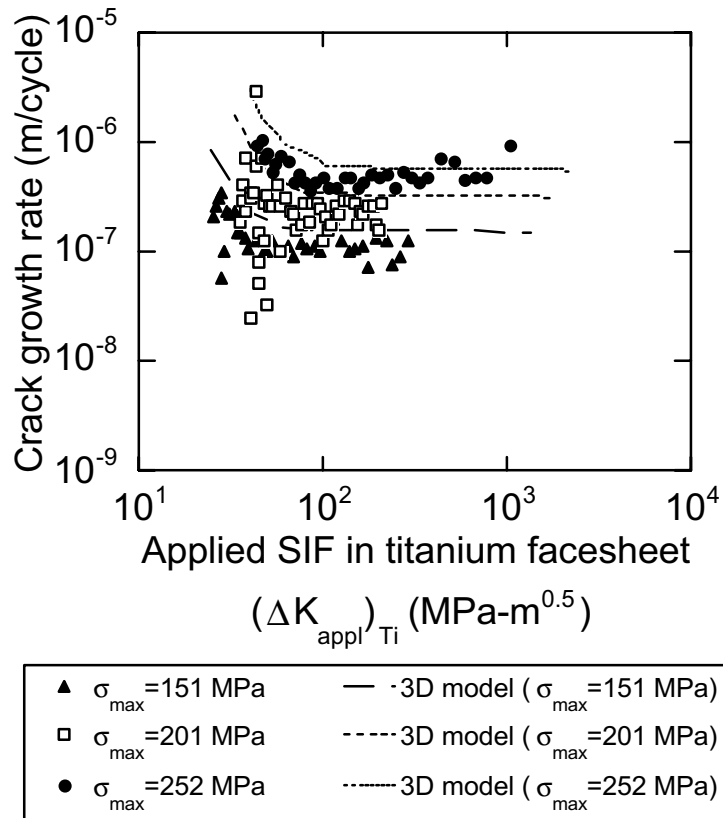


Figure 7. Comparison of model predictions and experimental data for $(\text{Ti}/90/0/90)_s$ loaded at three stress levels, $R = 0.1$.

Figure 8 displays results of the fatigue experiments conducted on $[\text{Ti}/0/90/\pm 30]_s$ laminates. Similar to the two laminates discussed above, the $[\text{Ti}/0/90/\pm 30]_s$ laminates exhibit an initially decreasing crack growth rate that becomes constant as the crack extends. For the same applied facesheet stress, the steady-state crack growth rate is slightly lower than that of the base $[\text{Ti}/0/90/0]_s$ laminate. The prediction of the 3D VCCT model is not in good agreement with the experimental results. The 3D VCCT model predicts a higher steady-state growth rate compared to the experimental results and the tunneling model predicts a lower steady-state growth rate compared to the experimental results. It is presumed that the presence of additional damage modes, particularly delamination within the composite core, reduces the accuracy of the model.

Overall, for cases where face-sheet cracking accompanied by delamination is the dominant failure mode, the modeling scheme outlined herein provides a good prediction of the experimental data. The effect of load level is well described as is the tendency for all the laminates investigated to exhibit a steady-state crack growth behavior as the crack length increases.

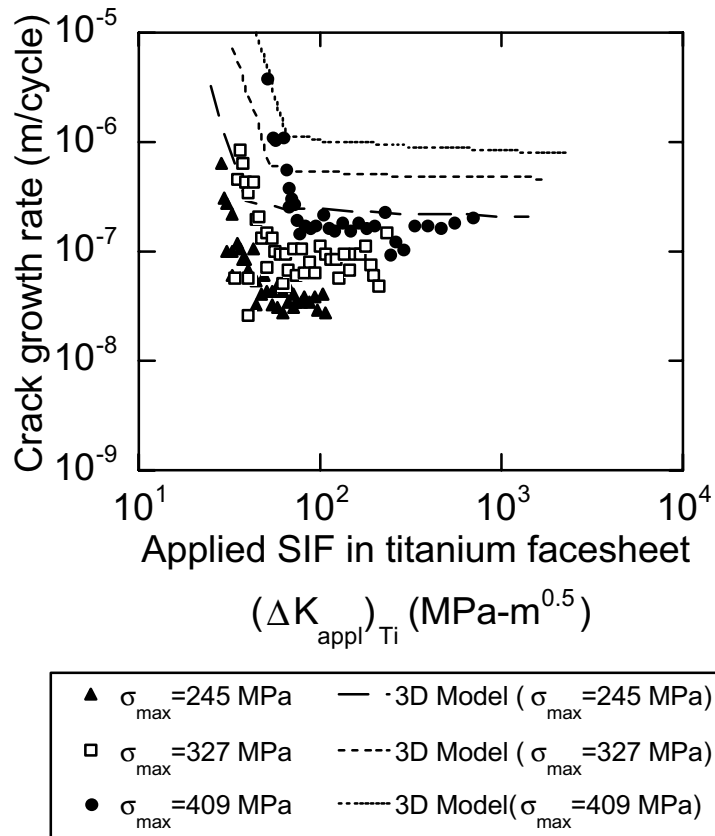


Figure 8. Comparison of model predictions and experimental data for $(Ti/0/90/\pm 30)_s$ loaded at three stress levels, $R=0.1$.

CONCLUDING REMARKS

A 3-D finite element model was constructed for face-sheet cracks in metal-composite hybrid laminates growing in combination with delamination between the facesheet and the composite core. Using the virtual crack closure technique the stress intensity factor at the crack tip was calculated. These results were compared to 2-D model results and discrepancies were identified, indicating that caution must be exercised in applying 2-D models to inherently 3-D problems.

The 3-D FE VCCT model was applied in conjunction with an experimentally determined Paris Law relationship to predict fatigue crack growth in titanium-graphite hybrid laminates. A good prediction of the experimental data was obtained for $(Ti/0/90/0_2)_s$ and $(Ti/90/0/90_2)_s$ laminates. A poorer prediction was obtained for a $(Ti/0/90/\pm 30)_s$ laminate, which is attributable to the presence of additional damage modes. In all cases a steady state crack growth behavior was attained, in which the crack growth rate was independent of the crack length. In all cases the TiGr laminates showed greatly reduced fatigue crack growth rates from that which would be expected for the monolithic titanium alloy, which when combined with the high specific strength and stiffness of TiGr suggests that it has good potential in aerospace applications.

ACKNOWLEDGEMENTS

This work was funded by NSF CAREER Award (CMS-9702399). The authors are very grateful for the help and support of the HSCT group at The Boeing Company. In particular, Ron Zabora, Bill Westre, Antonio Rufin, Elaine Worden, Matthew Miller, Eric Sager, and Edward Li. Technical discussions with Dr. Antonios Giannokopolous are gratefully acknowledged. In addition, experimental assistance was provided by John Kane, David Pinson, and Michelle Park.

REFERENCES

1. Burianek, D.A. and Spearing, S.M., "Delamination Growth from Facesheet Seams in Titanium-Graphite Hybrid Laminates." proceedings of *The 14th Tech. Conf. on Comp. Mat.*, 1999.
2. Burianek, D.A. and Spearing, S.M., "Fatigue Damage in Titanium-Graphite Hybrid Laminates," in the proceedings of *The 39th AIAA/ASME/ASCE/AHS/ASC Structures, Structural Dynamics, and Materials Conference*, 1998. AIAA-98-1959
3. Marissen, R. "Fatigue crack growth in ARALL, A hybrid aluminium-aramid composite material: Crack growth mechanisms and quantitative predictions of the crack growth rates," Ph.D. thesis, Delft University of Technology, 1984.
4. Lin, C.T. and Kao, P.W., "Delamination Growth and Its Effect on Crack Propagation in Carbon Fiber Reinforced Aluminum Laminates Under Fatigue Loading," *Acta Metall.*, Vol. 44, No. 3, 1996, pp. 1181-1188.
5. Guo, Y.G. and Wu, X.R., "Theoretical Model For Predicting Fatigue Crack Growth Rates In Fibre-Reinforced Metal Laminates," *Fat. Frac. Eng. Mat. Struc.*, Vol. 21, 1998.
6. Burianek, D. A., Giannakopoulos, A. E., and Spearing, S. M. "Modeling of Facesheet Crack Growth in Titanium-Graphite Hybrid Laminates, Part I, submitted to Engineering Fracture Mechanics, March 2001.
7. Burianek, D. A., and Spearing, S. M. "Modeling of Facesheet Crack Growth in Titanium-Graphite Hybrid Laminates, Part II, Experimental results, submitted to Engineering Fracture Mechanics, March 2001.
8. Burianek, D. A., "Mechanics of Fatigue Damage in Titanium-Graphite Hybrid Laminates" Ph.D Thesis, MIT March 2001.